DEVELOPMENT OF A HYBRID MUSCLE CONTROLLER FOR AN ACTIVE FINITE ELEMENT HUMAN BODY MODEL IN LS-DYNA CAPABLE OF OCCUPANT KINEMATICS PREDICTION IN FRONTAL AND LATERAL MANEUVERS

Oleksandr V. Martynenko
Fabian T. Neininger
Syn Schmitt
Institute for Modelling and Simulation of Biomechanical Systems,
Stuttgart Research Center for Simulation Sciences, University of Stuttgart
Germany

Paper Number 19-000215

ABSTRACT

Automotive safety has made a definite shift towards the continually increasing use of active safety systems in standard and highly automated vehicles (HAV) with a crucial need for the development of tools to supplement the assessment of such systems. Finite Element Human Body Models (FE HBMs) emerge as an innovative pre-requisite for this process in a virtual toolchain. Traditional passive HBMs were developed for in-crash simulations and are not suitable for straightforward use in the pre-crash phase because of inappropriate soft tissues response in low gravity scenarios and the absence of active muscle elements with a proper controller.

The current contribution covers some transformation issues from passive to active behavior for HBM and focuses on the development of a physiologically motivated controller for the whole HBM utilizing standard LS-DYNA keywords. The controller operates with the contraction dynamics of *MAT_MUSCLE material (also referenced as *MAT_156) through Hatze's activation dynamics and is capable of resembling a valid occupant response during maneuvers.

The proposed neural control model is a form of intermittent control and based on the assumption that the central nervous system governs the controlled motion through shifting between particular states of the musculoskeletal system – so-called "equilibrium points", where equilibrium of all acting external and internal forces is presumed for a resulting desired position. A hybrid formulation of the controller allows for taking closed-loop muscle stimulation (target muscle lengths "λ") as well as open-loop stimulation ("α") into account.

Previous to the whole body application, the equilibrium point hybrid controller (EPHC) approach was validated separately for some parts of the body only. Posture control capability was investigated by tracking motion speed, maximum muscles activation level and the effect of co-contraction. Subsequently, the full HBM simulations were carried out for lane change and 1g braking scenarios retrieved from the experimental database of the Occupant Model for Integrated Safety Project (OM4IS). A modified Total HUman Model for Safety (THUMS) model was correlated to a matched size volunteer with the comparison of head and torso excursions to appropriate experimental corridors.

Each single body region model was validated with in vivo kinematics and dynamics enabling an integration of the single body parts into the entire HBM. Measured maximal deviations for the whole HBM reside within the experimental corridors and correlate well with the volunteer.

The proposed approach permits modeling of active and reactive human responses with the help of an existing passive FE HBM after adequate adaptation of the model, muscle elements insertion and controller parameters tuning. Such model paves the way for the evaluation of new HAV interior concepts and the development of advanced vehicle safety systems.

INTRODUCTION

Crash tests with anthropometric test devices were historically inevitable for the design and test of automotive safety systems. However, stunningly fast development in simulation technologies not only increased computational power and simulation speed but also led to better, more valid digital models for studying the crash scenarios. The idea of using virtual human body models (HBM) emerged as a consequence of such advances realizing the benefits of virtual tests with higher biofidelity, compared to the commonly used virtual dummy models. Today, HBMs provide a vast application field in automotive safety system development, more and more penetrating from the in-crash phase studies into the pre-crash considering active human behavior, e.g., reflexes and simple movements.

As the primary simulation method nowadays in the automotive industry is the finite element (FE) analysis, regularly used state-of-the-art HBMs were implemented applying FE tools and validated for in-crash scenarios, basing mostly on the cadaver studies implying high loads during impact. Accordingly, such models are passive by their nature and are not suitable for straightforward application in the pre-crash phase for two main reasons: inadequate soft tissue response in low g scenarios and absence of active muscle elements with appropriate biological muscle controller. We hypothesize that it is possible to simulate active and realistic human motion with the currently available human body models after accurately solving these issues.

It is proven that muscle activity has a significant impact on the occupant kinematics during typical pre-crash events including braking or evasive maneuvers [1-3]. In recent years, there has been an increasing amount of literature on the aHBM development using different types of models and implementing different muscle activation strategies [4]. However, the number of the existing whole body FE aHBMs is still limited. THUMS v.5 model with a proportional-integral-derivative (PID) muscle controller including two controls for 16 three-dimensional joint angles and two reaction forces from a steering wheel and pedals was introduced in [5]. SAFER A-HBM model [6], which is based on the earlier THUMS v.3 [7], uses similar PID feedback controllers, but limited to seven relative angles between body parts. In contrast to mentioned models, λ-controller was adopted in reactive THUMS-VW model [8] to control around 600 muscles governed by 66 separate controllers. Despite the long development process and validation with many test cases these models still have some drawbacks in simulations of the whole crash sequence, with the main reason being lack of the omni-directionality. Consequently, there is a clear need for further developments of whole body aHBM with omni-directional controllers capable of combined maneuvers simulations.

The purpose of this study is the application of the macroscopic Hill-type [9] muscle modeling approach to activate a modified FE HBM also based on the THUMS v.3 [7]. Currently, such models reveal high joint and tissue stiffnesses which first have to be reduced. Henceforth this model was used with the aim to perform a simulation predicting occupant kinematics behavior according to the experimental data from the Occupant Model for Integrated Safety (OM4IS) project [1]. The hybrid equilibrium point controller (hybrid controller) proposed in [10] was adopted as a muscle control strategy including physiological Hatze's activation dynamics [11] interacting with contraction dynamics from the *MAT_MUSCLE in LS-DYNA R7.1.3 software [12]. All functions serving the controller needs were implemented inside LS-DYNA utilizing standard keywords to increase industrialization possibilities.

METHODS

Adaptation of the soft tissue response

One of the main prerequisites for active human body models (aHBM) is an adequate soft tissue response in low g load scenarios which are predominant in the pre-crash phase. As mentioned above, passive HBMs are found to be excessively stiff. Thus, 50^{th} percentile average occupant THUMS v.3 model was modified according to the procedure described in details in [13] to reproduce passive "relaxed" human occupant behavior with not active muscle elements included to fit experimental corridors given in [1]. According to the given study, "relaxed" state means fitting the corridor defined by displacement of the head center of gravity (CG) from volunteers with minimal muscle activity during 1 g braking loading pulse. The model adaptation includes mesh refinement in several body regions, a modification of connections between skin and some other parts, and the revision of the elastic modulus for specific soft tissues within physiological limits given in the literature.

Implementation of the biological muscle controller

Hybrid Equilibrium Point Controller: The neural control model used in this contribution is a form of intermittent control [14]. It is based on the assumption, that the controlled motion is governed by the central nervous system (CNS) through shifting between individual states of the musculoskeletal system (so-called "equilibrium points", EPs). In such an EP the equilibrium of external and internal forces acting on the body is reached resulting in the desired body posture. For the hybrid EP control approach [10,15], the motor command consists of two terms:

λ part – closed-loop feedback controller signal: Is based on the control of each of the body muscles target lengths. It could be known to the CNS by mapping of joint angles to associated muscles and could be stored in the memory as the magnitude of a respective signal from muscle spindles and Golgi tendon organs and obtained through learning process during an ontogenesis [16,17].

α part – open-loop feedforward controller signal: Could be generated directly by the CNS to compensate existing external loads, to hold the desired body posture or to reach a certain position in a specific manner, e.g. very fast, and could be governed via visual feedback or other internal sensors not directly associated with the muscle itself [18].

Herewith, the total neuronal stimulation signal from the CNS could be defined mathematically as a combination of the closed-loop signal and open-loop signal (Equation 1). Signal values are varying inside the interval [0...1], where "0" is no muscle stimulation at all and "1" is a fully stimulated muscle. It should be noted here, that full stimulation is a theoretical upper limit, and maximum voluntary stimulation is below "1".

$$u_{hybrid}^{total}\Big|_0^1 = u_{\lambda}^{closed} + u_{\alpha}^{open} \qquad \text{(Equation 1)}$$

To simplify the use of this method in industrial applications and to allow for intuitive and easy handling, the controller code was implemented within LS-DYNA software using standard keywords *DEFINE _FUNCTION, *DEFINE_CURVE and *DEFINE_CURVE_FUNCTION in combination with C programming language for missing functionality. Since LS-DYNA provides no capabilities presently to solve user specified differential equations directly inside the program code, a prescribed velocity of the specially created nodes (*BOUNDARY_PRESCRIBED_MOTION keyword) was used for retaining old variable values from the previous load step, which are needed for numerical integration over time and muscle neural delay implementation. A flowchart of the controller logic and its incorporation in combination with the LS-DYNA muscle material model *MAT_MUSCLE is presented in Figure 1, where α represents the open-loop part of the controller signal, and not the α motor neuron signals. Other corresponding symbols could be found in Table 1.

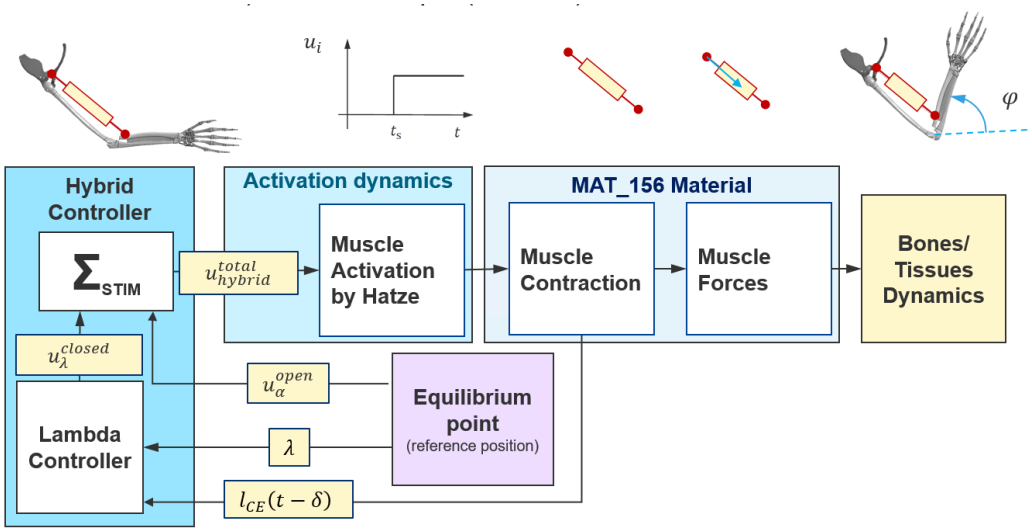

Figure 1. Flowchart of the muscle controller code shown for the single muscle element only.

As seen from the given chart, the implemented controller uses delayed actual muscle length value $l_{CE}(t-\delta)$ as a feedback signal compared to the target length of the muscle λ and a predefined stimulation u_{α}^{open} as a feedforward signal. Both inputted values of λ and u_{α}^{open} are defined by the equilibrium point (reference position) given in the simulation time and were retrieved from existing experimental data [1] a priori to simulation runtime.

Muscle length signal has a delay due to the time of sensory impulse traveling from muscle spindle through the nerve to the control center and back. The muscle spindle belongs to the group of proprioceptors and corresponds to the organ of perception inside the muscle belly. This organ has the functionality similar to a closed-loop PD-controller because muscle tissue itself shows visco-elastic behavior [10]. Thus, the equation of the λ-controller part could be written in the following form (Equation 2) with the corresponding symbols shown in Table 1.

$$u_{\lambda}^{closed}\Big|_0^1 = \frac{k_p}{l_{CEopt}} \cdot [l_{CE}(t-\delta) - \lambda] + \frac{k_d}{l_{CEopt}} \cdot v_{CE}(t-\delta) \qquad \text{(Equation 2)}$$

From the given relation it is evident that deviations in targeted and actual muscle lengths in connection with the contraction speed result in increased muscle stimulation. The main advantage of λ-control is that the forces needed to reach a target position are calculated during the motion, and no inverse problem has to be solved. Thus, switching between different intermediate postures during simulation time is done by changing the muscle's target lengths without any modifications in the controller code. This allows intuitive and easy handling in industrial applications.

Table 1.
List of the Parameters and Corresponding Symbols Used Within the Controller Code

Symbol	Parameter Definition	Value
t	Current simulation time	Calculated in runtime
δ	Neural delay of the muscle signal	Preset value
v_{CE}	Contraction velocity of the contractile element (muscle fiber)	Calculated in runtime
l_{CE}	Actual length of the contractile element (muscle fiber)	Calculated in runtime
l_{CEopt}	Optimal length of the contractile element (muscle fiber)	Preset value
λ	Target length of the muscle	Preset value
k_p	Proportional controller gain	Preset value
k_d	Differential controller gain	Preset value
γ	Free calcium ion concentration in the muscle	Calculated in runtime
$\dot{\gamma}$	Time derivative of free calcium ion concentration	Calculated in runtime
γ_{min}	Initial calcium ion concentration	Preset value
u_{hybrid}^{total}	Total muscle stimulation level from the controller	Calculated in runtime
u_{λ}^{closed}	Stimulation signal from closed-loop feedback controller part	Preset value
u_{α}^{open}	Stimulation signal from open-loop feedforward controller part	Preset value
a	Muscle activation level or activity	Calculated in runtime
a_{min}	Minimal muscle activation level	Preset value

Activation Dynamics: Physiological muscle activation dynamics introduced in [11] is used for a transfer of the total stimulation signal u_{hybrid}^{total} from the Hybrid controller into muscle activation level a, which could be directly inputted as a constant value or a continuous function (load curve) to LS-DYNA material *MAT_MUSCLE. The activation signal is calculated in the controller code in two steps: 1) the free calcium ion concentration is calculated by an integration of a first-order differential Equation 3 with an explicit Euler scheme (Equation 4); 2) this result is fed afterwards in an Equation 5 to calculate the resulting muscle activation with relation to renormalized factor for length dependency.

$$\dot{\gamma} = m \cdot (u - \gamma) \qquad \text{(Equation 3)}$$

where $m = 0.01\ (1/ms)$ – Hatze's activation frequency constant.

$$\gamma_{n+1} = \gamma_n + \dot{\gamma}_n \cdot dt \quad \text{(Equation 4)}$$

taking into account $\gamma(0) = \gamma_{min}$.

$$a(t) = \frac{a_{min} + [\rho(l_{CErel}) \cdot \gamma(t)]^{\nu}}{1 + [\rho(l_{CErel}) \cdot \gamma(t)]^{\nu}} \quad \text{(Equation 5)}$$

where $\rho(l_{CErel}) = \rho_c \cdot \frac{l_\rho - 1}{l_\rho / l_{CErel} - 1}$ is Hatze's length dependency function with respective constants $\rho_c = 9.10$, $l_\rho = 2.9$ and $\nu = 2.0$ taken from [19].

Contraction Dynamics: The muscle's contraction dynamics is incorporated into LS-DYNA material *MAT_MUSCLE [12] and generates active force from contractile element according to the law shown in the Equation 6.

$$F_{CE} = \sigma_{max} \cdot a(t) \cdot f_l(l) \cdot f_v(v) \quad \text{(Equation 6)}$$

where σ_{max} – is a generated peak stress for the muscle, $a(t)$ – is a muscle activation level calculated in the Equation 5, $f_l(l)$ – is a force-length relation in the exponential form taken from [15] and $f_v(v)$ – is a force-velocity relation in a hyperbolic form also from [15] (Figure 2). Additionally, the force generated by the muscle finite element is influenced by passive and damping components. The values of generic parameters used in *MAT_MUSCLE for all muscles along with appropriate references are reported in Table 2 below.

Table 2.
Generic Muscle Parameters for LS-DYNA Material *MAT_MUSCLE

Parameter	Description	Value (units)	Source
PIS	Peak Isometric Stress	0.001 (GPa)	[20]
SRM	Maximum Strain Rate	0.005 (ms-1)For Hand muscles	[21]
		0.0022 (ms-1) For Torso and Neck muscles	[21]
SVS	Force-Length Relation	Load curve Input	[15]
SVR	Force-Velocity Relation	Load Curve Input	[15]
SSP	Stress vs. the Stretch Ratio	Load Curve Input	[15]

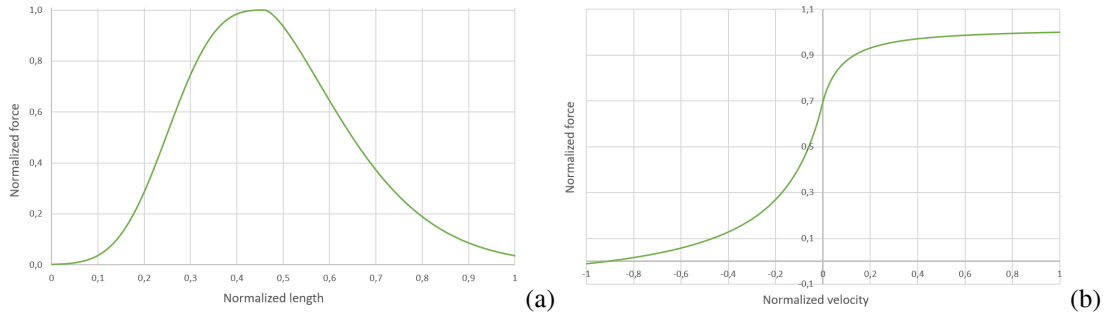

(a) (b)

Figure 2. Force-length (a) and force-velocity (b) relations used for all muscles according to [15].

Insertion of the muscle elements into the HBM

About 370 muscles from the human body were added subsequently into aHBM for the current study. Among them: 180 muscles were added to the neck, 150 – to the thoracic region and 40 – to upper extremities. All these muscles are represented by one-dimensional truss elements (*ELEMENT_BEAM, formulation ELFORM=3) with assigned material *MAT_MUSCLE. In order to give them the necessary anatomical and physiological properties such as origin and insertion nodes, optimal muscle length and physiological cross-sectional area (PCSA), these values were obtained from complementary literature sources [22-25].

Occupant Model for Integrated Safety Project Experimental Data

OM4IS project major objective was to gather a comprehensive collection of vehicle and occupant kinematic data based on results from human volunteers seated in the passenger position undergoing different driving maneuvers. Among them were emergency braking from two different speeds, lane change maneuvers to both sides and combined ones. This data was published in several sources prior to our study and represents an excellent base for the aHBM validation. Load□case results for emergency braking from 50 km/h and lane change, where a combination of lateral and frontal accelerations occurred, given in [1] are used in this contribution to validate the whole body model.

RESULTS

Validation at the body region level

To validate the proposed hybrid controller a simple multibody musculoskeletal model similar to the one proposed in [10] was built. This model consists of three rigid bodies including bones and eight truss elements representing muscles (4 flexors and 3 extensors) which actuate the elbow joint. The elbow flexion movement from 45deg to 145deg was simulated according to the given test set-up. This experimental source was taken because it offers a clear test setup, which is easy to reproduce in a simulation environment. Additionally, only one joint is actuated which allows a fine-tuning of the controller parameters. The resultant model was retrieved from THUMS model [7] by separating the bone parts and adding a revolute joint for the elbow with the stiffness of 0.6 kN·mm/rad specified according to [21] (Figure 3). A physiological muscle routing was not implemented, hence a supplementary rigid beam with the total length of 20mm was connected to the ulna bone to enable the triceps muscle elements connection.

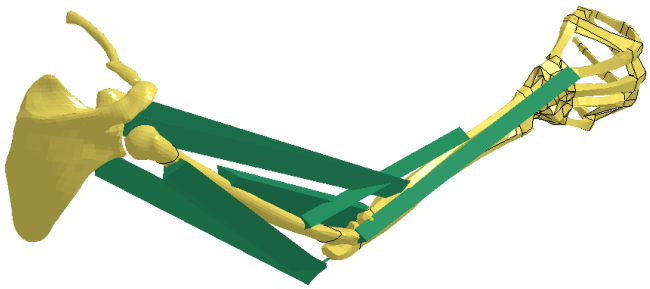

Figure 3. Multibody arm model with inserted muscles.

The structure of the hybrid controller includes feedforward and feedback components. Therefore, input signals for both have to be set.

Deriving control signals for the feedforward α part: Open-loop stimulation signal is governed directly by the CNS to switch between EPs and in current study intended mainly to hold the position or to compensate existing external loads by the muscle co-contraction. By definition, the static equilibrium is considered in any of the EPs resulting in constancy of the angular velocity and acceleration which should be equal to zero [15] (Equation 7).

$$\dot{\varphi}_i = 0 \text{ and } \ddot{\varphi}_i = 0 \quad \text{(Equation 7)}$$

These equalities could be rewritten in a form of moment equilibrium over the joint

$$\sum_{i=1}^{n} M_i = 0 \quad \text{(Equation 8)}$$

For the case when external loading is absent, taking into account definitions of the muscle moment $M_i = \vec{r}_i \cdot \vec{F}_i$, moment arm $r_i(\varphi) = \frac{\partial l_{Mus,i}}{\partial \varphi}$ and linear force from the element with *MAT_MUSCLE material $F_i = a_{i,\alpha} \cdot PCSA_i \cdot \sigma_{max} \cdot (\sigma_{SVS} + \sigma_{SSP})$ the equation for finding muscle activation levels $a_{i,\alpha}$ for α part of the hybrid controller could be derived:

$$\sum_{i=1}^{n} \left(\frac{\partial l_{Mus,i}}{\partial \varphi} \cdot a_{i,\alpha} \cdot PCSA_i \cdot \sigma_{max} \cdot (\sigma_{SVS} + \sigma_{SSP})\right) = 0 \text{ (Equation 9)}$$

This system of linear equation of n variables for muscle activation levels $a_{i,\alpha}$ could be solved for stimulation levels $u_{i,\alpha}^{open}$, which would be used as an input signal for the controller, by coupling it with the Equations 3 and 5. It results in a manifold of solutions, that could be constrained by applying additional conditions governed by the desired co-contraction in the muscles defining the respective joint stiffness. Higher co-contraction (muscle activation levels) leads to higher apparent joint stiffness slowing the movement velocities and vice versa. A list of all symbols with definitions used in the calculations is given in Table 3.

Table 3.
List of Symbols Used in Calculations

Symbol	Definition	Value
M_i	Moment generated by the muscle	Calculated in runtime
r_i	Instantaneous moment arm of the muscle	Calculated in runtime
F_i	Force generated by the muscle	Calculated in runtime
$l_{Mus,i}$	Length of the muscle	Derived in range of motion
φ_i	Joint angle	Preset value
$\dot{\varphi}_i$	Angular velocity of the joint	Calculated in runtime
$\ddot{\varphi}_i$	Angular acceleration of the joint	Calculated in runtime
$u_{i,\alpha}^{open}$	Muscle stimulation level from the feedforward α controller	Calculated in runtime
$a_{i,\alpha}$	Activation corresponding to the $u_{i,\alpha}^{open}$	Calculated in runtime
$PCSA_i$	Physiological cross sectional area of muscle	Calculated in runtime
σ_{max}	Peak isometric stress	Calculated in runtime
σ_{SVS}	Normalized stress generated by contractile element	Read from SVS curve
σ_{SSP}	Normalized stress generated by parallel elastic element	Read from SSP curve

Deriving control signals for the feedback λ part: The closed-loop stimulation signal in real muscle builds on the interaction of muscle spindles and Golgi tendon organs from the sensory side and α- and γ- motoneurons from the actuator side. From the technical perspective, such a system is based on the PD feedback control with the target to maintain the desired muscle length (Equation 2). Thus, before any analysis, it is crucial to preset the target muscle length as a variable for the controller to function. The straight forward way to find these values is to run the pre-simulation that brings the model into the desired state and measure the obtained muscle elements length knowing the attachment nodes. Such procedure was done for the arm model built and elbow flexion from 45deg to 145deg. Target length obtained and applied in the simulation for different muscles over time are shown in Figure 4.

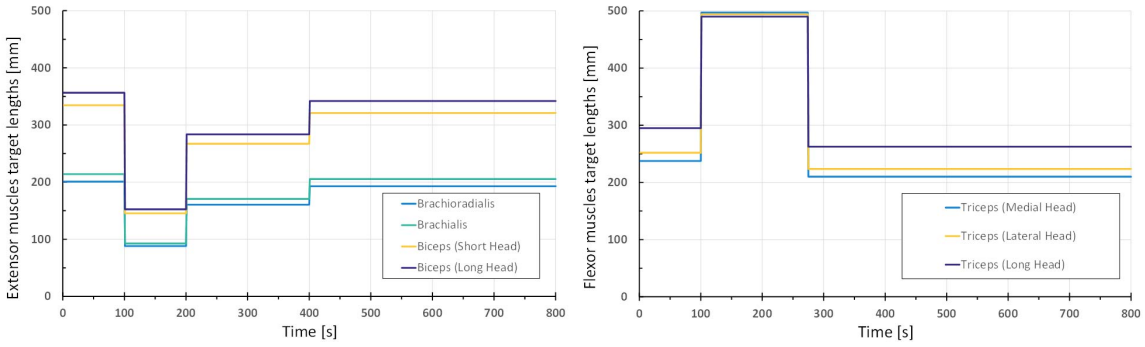

Figure 4. Muscle target lengths (feedback controller input signals λ) used for flexor and extensor muscles.

Simulation results for the arm model: FE arm model simulation results show a good correlation with the volunteer kinematics (Figure 5). A mismatch in a joint stiffness of the multi-body model compared to the human arm could explain small difference in a curve slope, thus higher speed of the simulated movement. Likewise, the lower joint stiffness in the model can also be a reason for a broader range of joint angles achieved.

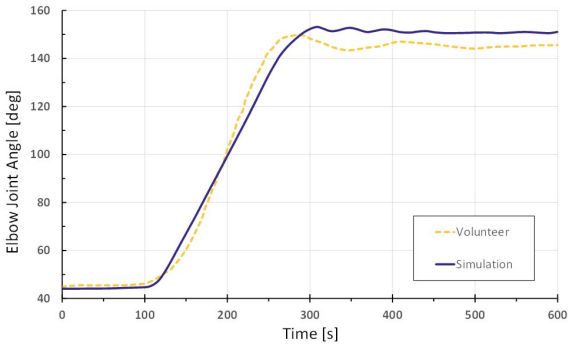

Figure 5. Comparison of elbow joint kinematics for the hybrid controller and volunteer response from [10].

Validation at the HBM level

After successful validation at the body region, the level of the study was extended to the whole HBM level. As a validation basis volunteer tests conducted in the OM4IS project [1] described shortly above was used. Braking and lane change scenarios were chosen for the current study. Data available for the comparison includes vehicle acceleration, head (at ear level) and torso (at T5 level) excursions. A model setup that is similar to the real world test was represented in the simulation environment. AHBM with seatbelt applied is seating in the reference seat in front passenger occupant position with the corresponding maneuver motion pulse applied (Figure 6).

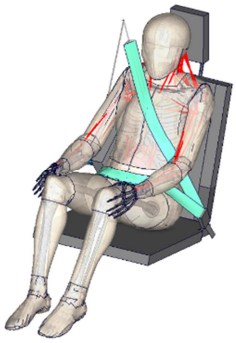

Figure 6. Simulation setup for the sled tests.

Open-loop stimulations $u_{i,\alpha}^{open}$ capable of maintaining the sitting posture with muscle co-contraction were determined and input, following by automatic calculation of closed-loop stimulation $u_{i,\lambda}^{closed}$ according to the procedure described above depending on the validation case.

Emergency braking: Following the experiment, a deceleration pulse to zero of the vehicle with the initial velocity of 50 km/h was applied to the sled. Feedback λ-controller was activated starting from the 10% of the peak pulse value and attaining 80-90% of the initial muscle length set as targets in the most distant body deflections. Choice of the muscle target lengths λ was performed according to suggestions given in [16].

Simulation results carried out for whole HBM with the functioning controller (referenced as active HBM) and without it (referenced as passive HBM) are shown in Figure 7. Head and torso centers of gravity (CG) excursions in the sagittal plane of the body were measured and compared to the experimental corridors. As seen from the results, almost for the whole observed maneuver time the aHBM excursions are lying inside the corridor measured for volunteers, being outside after HBM's contact with the seat on the ending phase. It could be explained by the influence of the contact parameters between the model's back and seat surface, which need to be tuned more precisely. Passive HBM is outside of the corridor for the initial phase and close to the margin later, having the same problem with a contact in the end.

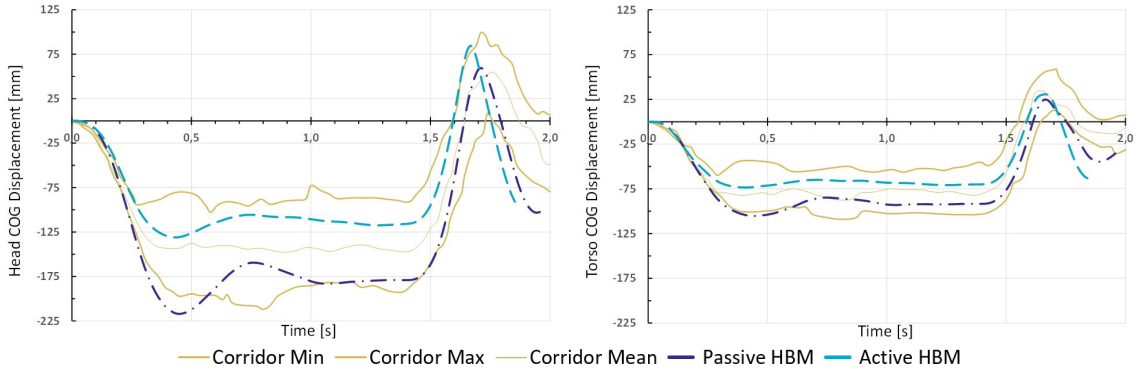

Figure 7. Comparisons of head and torso CG excursions during emergency braking maneuver and volunteer response corridor from [1].

Lane change: Lateral acceleration pulse of the vehicle with the longitudinal velocity 50km/h was applied to the sled. Feedback controller was active from the start and muscle target lengths λ were reversed at the point where the acceleration changes its direction with the pulse slope 0.

Simulation results are available in Figure 8, where head and torso CG excursions in the coronal plane of the body compared to the experimental corridors are given. In the same way, as observed for previous validation case, aHBM has less excursions with respect to the measurement corridor compared to a passive one. Due to the λ controller advantage to control each muscle length individually, additional volunteer muscle activity in order to avoid contact with the B-pillar was mimicked correctly. Head excursion being severely out of the corridor could be explained by the absence of physiological muscle routing in the neck, which is addressed in the DISCUSSION. Besides, more accurate assignment of target lengths to muscle groups responsible for neck flexion and lateral flexion of the lumbar spine could improve the aHBM kinematics. Further studies are needed in this direction.

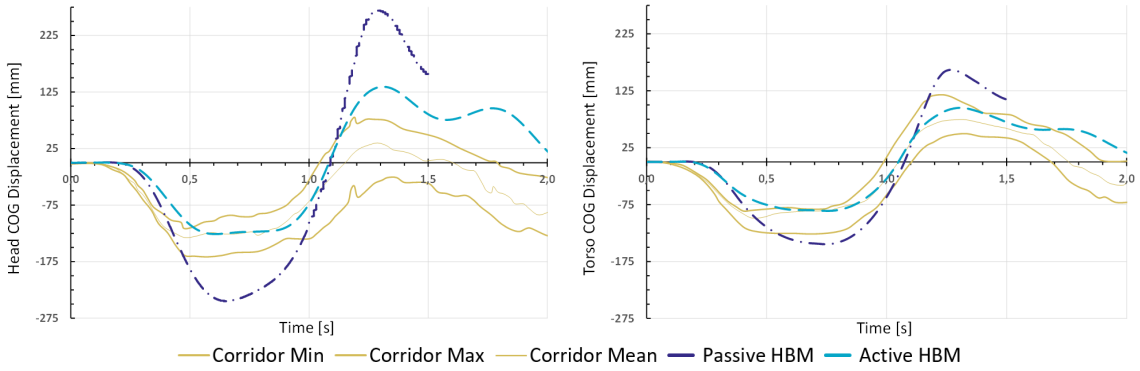

Figure 8. Comparisons of head and torso CG excursions during lane change maneuver and volunteer response corridor from [1].

DISCUSSION

The hybrid controller coupled with Hatze's activation dynamics represents physiological control of the muscle elements, which have been validated initially with an arm model. Obtained knowledge and original findings were extended to other body parts first and finally to the whole HBM. The suggested controller shows the capability to generate motion with appropriate muscle activation signals both in 1g braking and lane change scenarios, although the last one is considered to be a demanding task because of a switch in a muscle activity into opposite directions during the same event. This issue was successfully addressed with the proper combination of target lengths set to the muscles and governed by the hybrid controller, producing movements fast enough and similar to the volunteers.

As an additional outcome of the study, the importance of correct environment modeling according to the test protocol should be mentioned. The interior of the test vehicle should be replicated with all possible details since the seat and the seatbelt interact with the aHBM and produce additional contact forces and reactions, which affect the controller functioning.

Despite the good correlation with the experiments obtained, certain improvements need to be implemented in the aHBM and the hybrid controller. First of all, LS-DYNA material *MAT_MUSCLE that is currently used in a truss muscle elements lacks the serial elastic element representing elasticity of tendons, which was proven to have an important role for muscle modeling in some works [26,27]. Secondly, one of the current model limitations is the absence of muscle routing in some regions representing physiological muscle path including wrapping around joints. Such a modeling approach allows fulfilling of the correct line of action for the muscle, thus producing correct moment arms around the joints as shown in [28]. Thirdly, the current study does not include full activation calculation from the hybrid controller for the leg muscles, because the experimental data lacks the contribution of leg muscles in the motion studied in the study used [1]. Fourthly, the last conditionality applied in the current simulations is the absence of the gravity loading due to limitations of underlying passive HBM. Normally, due to the hybrid controller formulation, it would not affect the functioning itself, rather it will change the muscle activation levels produced and their correspondence for different muscle groups. These limitations designate trends for future work.

CONCLUSIONS

A further step towards an omnidirectional aHBM was made in this study. Such a model could be widely used for integrated safety systems development and accident whole sequence studies. Proposed physiological muscle activation hybrid controller is capable of resembling occupant kinematics in low-speed events, which was validated against experimental tests for 1g braking and lane change maneuvers from the OM4IS project. Besides, suggested control strategy allows to perform modeling of active and reactive human responses for other maneuvers by tweaking the controller parameters in conformity with the desired movement to be simulated. As a next ambitious goal one can set is a simulation of combined maneuvers where acceleration in two directions simultaneously is employed.

ACKNOWLEDGEMENTS

This work was supported by the German Research Foundation (DFG) within the Cluster of Excellence "Data-Integrated Simulation Science" (EXC 2075) at the University of Stuttgart and Tech Center i-protect.

The authors want to thank Atul Mishra, Pronoy Ghosh and Shubham Kulkarni for helpful discussions, useful advice, broad knowledge and valuable assistance with LS-DYNA simulations; Christian Mayer and Ravi Kiran Chitteti for comprehensive support and constructive collaboration.

REFERENCES

[1] Huber, P., Kirschbichler, S., Prüggler, A. and Steidl, T., 2015. “Passenger kinematics in braking, lane change and oblique driving maneuvers.” In Proceedings of the IRCOBI Conference (Lyon, France, September 9-11), 783-802.

[2] Muggenthaler, H., Adamec, J., Praxl, N. and Schönpflug, M., 2005. “The influence of muscle activity on occupant kinematics.” In Proceedings of the IRCOBI Conference, (Prague, Czech Republic, September 21-23), 313-323.

[3] Olafsdottir, J.M., Östh, J., Davidsson, J. and Brolin, K., 2013. “Passenger kinematics and muscle responses in autonomous braking events with standard and reversible pre□tensioned restraints.” In Proceedings of the IRCOBI Conference, (Gothenburg, Sweden, September 11-13), 602-617.

[4] Östh, J, Brolin, K, Ólafsdóttir, JM, Davidsson, J, Pipkorn, B, Jakobsson, L, Törnvall, F and Lindkvist, M., 2015. “Muscle activation strategies in human body models for the development of integrated safety.” In

Proceedings of the 24th International technical conference on the enhanced safety of vehicles (ESV), Gothenburg, Sweden.

[5] Kato, D., Nakahira, Y. and Iwamoto, M., 2017. "A study of muscle control with two feedback controls for posture and reaction force for more accurate prediction of occupant kinematics in low-speed frontal impacts." In Proceedings of the 25th International technical conference on the enhanced safety of vehicles (ESV), Detroit, USA.

[6] Östh, J., Brolin, K. and Bråse, D., 2014. "A Human Body Model with Active Muscles for Simulation of Pretensioned Restraints in Autonomous Braking Interventions." Traffic Injury Prevention, 16(3), 304–313.

[7] Iwamoto, M., Nakahira, Y., Tamura, A., Kimpara, H., Watanabe, I. and Miki, K., 2007. "Development of advanced human models in THUMS." In Proceedings of the 6th European LS-DYNA Users' Conference, Gothenburg, 47-56.

[8] Sugiyama, T., Weber, J., Sandoz, B. and Bensler, H.-P., 2018. "Validation of a Reactive Finite Element Human Body Model under Moderate Lateral Loading", In Proceedings of the 7th International Symposium on "Human Modeling and Simulation in Automotive Engineering," October 18-19, Berlin, Germany.

[9] Hill, A.V. "The heat of shortening and the dynamic constants of muscle" 1938. Proceedings of the Royal Society of London. Series B - Biological Sciences. The Royal Society, 126(843), pp. 136–195.

[10] Kistemaker, D. A., Van Soest, A. (Knoek) J. and Bobbert, M. F. 2006 ."Is Equilibrium Point Control Feasible for Fast Goal-Directed Single-Joint Movements?", Journal of Neurophysiology. American Physiological Society, 95(5), pp. 2898–2912.

[11] Hatze, H. 1977. "A myocybernetic control model of skeletal muscle." Biological Cybernetics. Springer Nature America, Inc, 25(2), pp. 103–119.

[12] LS-DYNA Keyword User's Manual Volume I, LS-DYNA R7.1 (r:5471). Livermore: Livermore Software Technology Corporation; May 26, 2014.

[13] Shelat, C., Ghosh, P., Chitteti, R. and Mayer, C., 2016. ""Relaxed" HBM–an Enabler to Pre-Crash Safety System Evaluation." In Proceedings of the IRCOBI Conference (Malaga, Spain, September 14-16), 239-247.

[14] Gawthrop, P., Loram, I., Lakie, M. and Gollee H., 2011. "Intermittent control: a computational theory of human control." Biological Cybernetics. Springer Nature, 104(1–2), pp. 31–51.

[15] Bayer, A., Schmitt, S., Günther, M. and Haeufle, D.F.B., 2017. "The influence of biophysical muscle properties on simulating fast human arm movements." Computer Methods in Biomechanics and Biomedical Engineering. Informa UK Limited, 20(8), pp. 803–821.

[16] Feldman, A. G. and Levin, M. F. 2009. "The Equilibrium-Point Hypothesis – Past, Present and Future." in Advances in Experimental Medicine and Biology. Springer US, pp. 699–726.

[17] Martynenko, O., Schmitt, S., Bayer, A., Blaschke, J. and Mayer, C., 2017. "A movement generation algorithm for FE Human Body Models." PAMM. Wiley, 17(1), pp. 201–202.

[18] Bizzi, E., Hogan, N., Mussa-Ivaldi, F.A. and Giszter, S., 1992. "Does the nervous system use equilibrium-point control to guide single and multiple joint movements?" Behavioral and Brain Sciences. Cambridge University Press (CUP), 15(4), pp. 603–613.

[19] Rockenfeller, R., Günther, M., Schmitt, S. and Götz, T., 2015. "Comparative Sensitivity Analysis of Muscle Activation Dynamics." Computational and Mathematical Methods in Medicine. Hindawi Limited, 2015, pp. 1–16.

[20] van der Horst, M.J., Thunnissen, J.G.M., Happee, R., van Haaster, R.M.H.P. and Wismans, J.S.H.M., 1997. "The Influence of Muscle Activity on Head-Neck Response During Impact." In: SAE Technical Paper Series, 12 November 1997. SAE International.

[21] Östh, J., Brolin, K. and Happee, R., 2012. "Active muscle response using feedback control of a finite element human arm model." Computer Methods in Biomechanics and Biomedical Engineering. Informa UK Limited, 15(4), pp. 347–361.

[22] Borst, J., Forbes, P. A., Happee, R. and Veeger, D., 2011. "Muscle parameters for musculoskeletal modeling of the human neck." Clinical Biomechanics. Elsevier BV, 26(4), pp. 343–351.

[23] Christophy, M., Faruk Senan, N.A., Lotz, J.C. and O'Reilly, O.M., 2011. "A Musculoskeletal model for the lumbar spine." Biomechanics and Modeling in Mechanobiology. Springer Nature, 11(1–2), pp. 19–34.

[24] Standring, S. Gray's anatomy: the anatomical basis of clinical practice. Philadelphia: Elsevier Limited, 2016.

[25] Östh, J., Brolin, K., Carlsson, S., Wismans, J. and Davidsson, J., 2012. "The Occupant Response to Autonomous Braking: A Modeling Approach That Accounts for Active Musculature." Traffic Injury Prevention. Informa UK Limited, 13(3), pp. 265–277.

[26] Kleinbach, C., Martynenko, O., Promies, J., Haeufle, D.F.B., Fehr, J. and Schmitt, S., 2017. "Implementation and validation of the extended Hill-type muscle model with robust routing capabilities in LS-DYNA for active human body models." BioMedical Engineering OnLine. Springer Nature America, Inc, 16(1).

[27] Günther, M., Schmitt, S. and Wank, V., 2007. "High-frequency oscillations as a consequence of neglected serial damping in Hill-type muscle models." Biological Cybernetics. Springer Nature, 97(1), pp. 63–79.

[28] Hammer, M., Günther, M., Haeufle, D.F.B. and Schmitt, S., 2019. "Tailoring anatomical muscle paths: a sheath-like solution for muscle routing in musculo-skeletal computer models." Mathematical Biosciences.